

## Electronic Supplementary Information for:

### Towards Emission Enhancement of Gold Nanoclusters Using Plasmonic Systems: Advantages and Limitations

Ondrej Pavelka<sup>1</sup>, Sergey Dyakov<sup>2</sup>, Klaudia Kvakova<sup>3</sup>, Jozef Vesely<sup>4</sup>, Petr Cigler<sup>3</sup>, Jan Valenta<sup>1</sup>

<sup>1</sup> Department of Chemical Physics and Optics, Faculty of Mathematics and Physics, Charles University, Ke Karlovu 3, 121 16, Prague, Czech Republic

<sup>2</sup> Photonics & Quantum Materials Center, Skolkovo Institute of Science and Technology, Nobel Street 3, Moscow 143025, Russia

<sup>3</sup> Institute of Organic Chemistry and Biochemistry of the Czech Academy of Sciences, Flemingovo nam. 2, 166 10, Prague, Czech Republic

<sup>4</sup> Department of Physics of Materials, Faculty of Mathematics and Physics, Charles University, Ke Karlovu 3, 121 16, Prague, Czech Republic

## 1. Synthesis and characterization of the nanoparticles

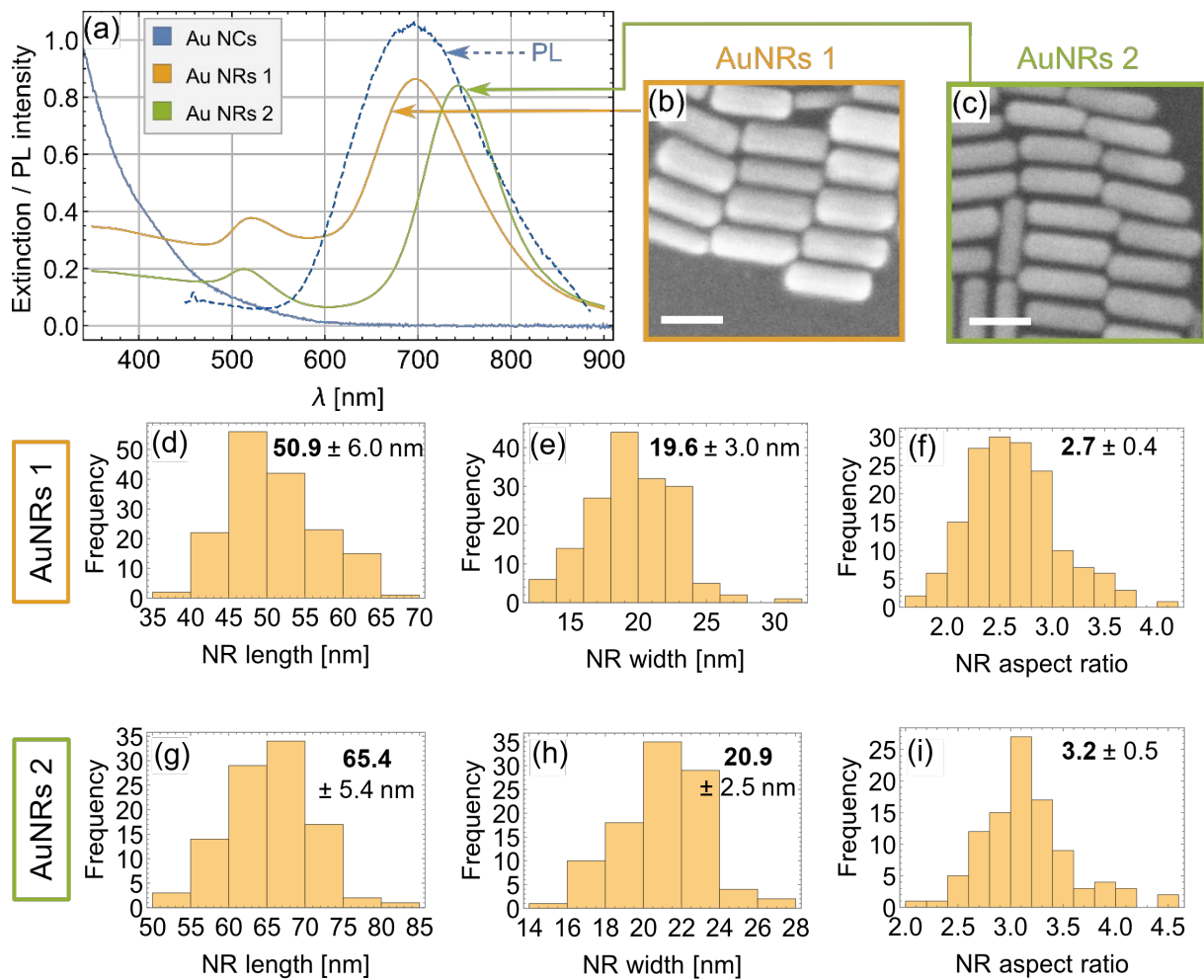


Figure S1: Structural characterization of the two types of AuNR samples used in the experiments. (a) The extinction spectra of AuNRs 1, AuNRs 2 and AuNCs (solid lines) and PL peak of AuNCs excited at 405 nm (dashed line). The spectra were normalized to highlight the spectral position of the important features – the vertical scale is therefore irrelevant. (b,c) SEM images of bare AuNRs 1 and AuNRs 2. The scalebar is 100 nm in both images. (d-f) Histograms of the measured dimensions of AuNRs 1 and (g-i) AuNRs 2. The results are presented as mean  $\pm$  standard deviation.

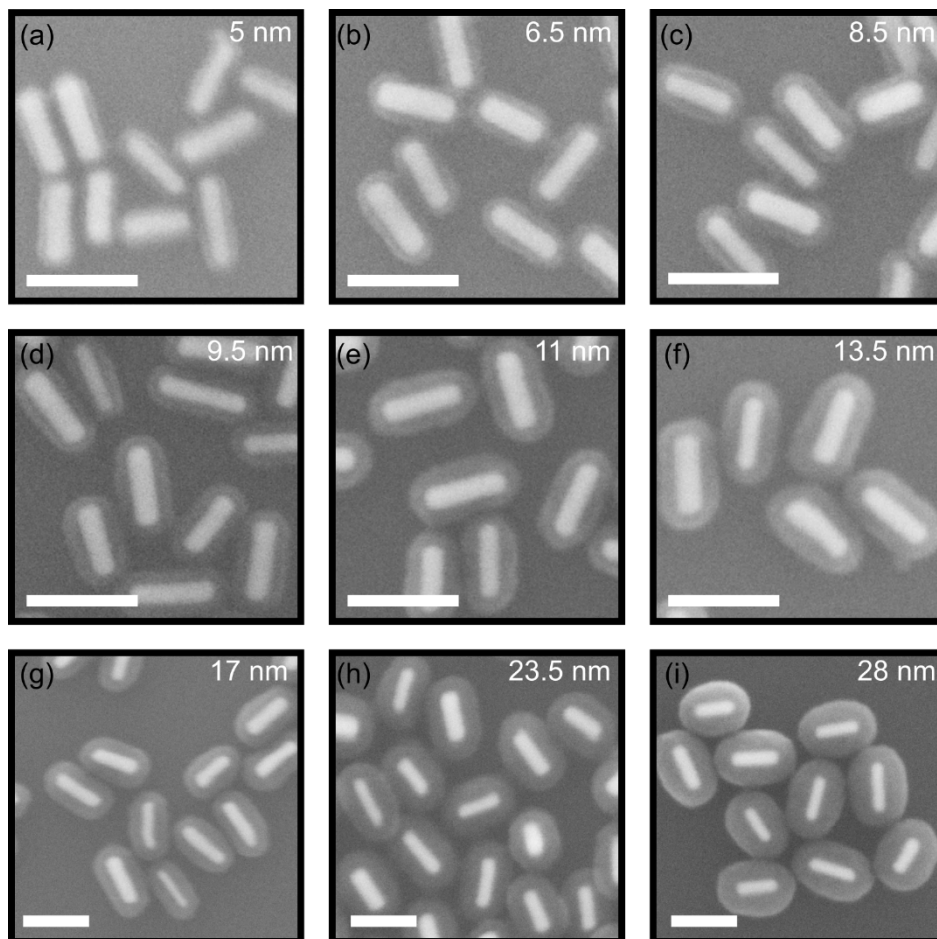


Figure S2: Representative SEM images of Au@SiO<sub>2</sub> NRs with different silica shell thicknesses prepared from AuNRs 2 (the corresponding thicknesses are shown in the upper right corner). All scalebars are 100 nm.

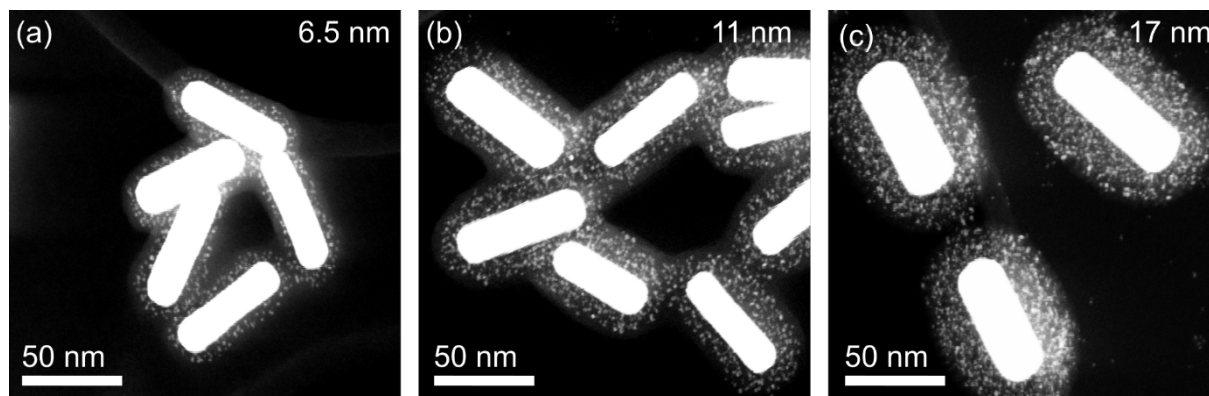


Figure S3: Representative HAADF-STEM images of AuNRs@AuNCs prepared from AuNRs 2 with different silica shell thicknesses (shown in the upper right corner).

## 2. Complementary PL measurements

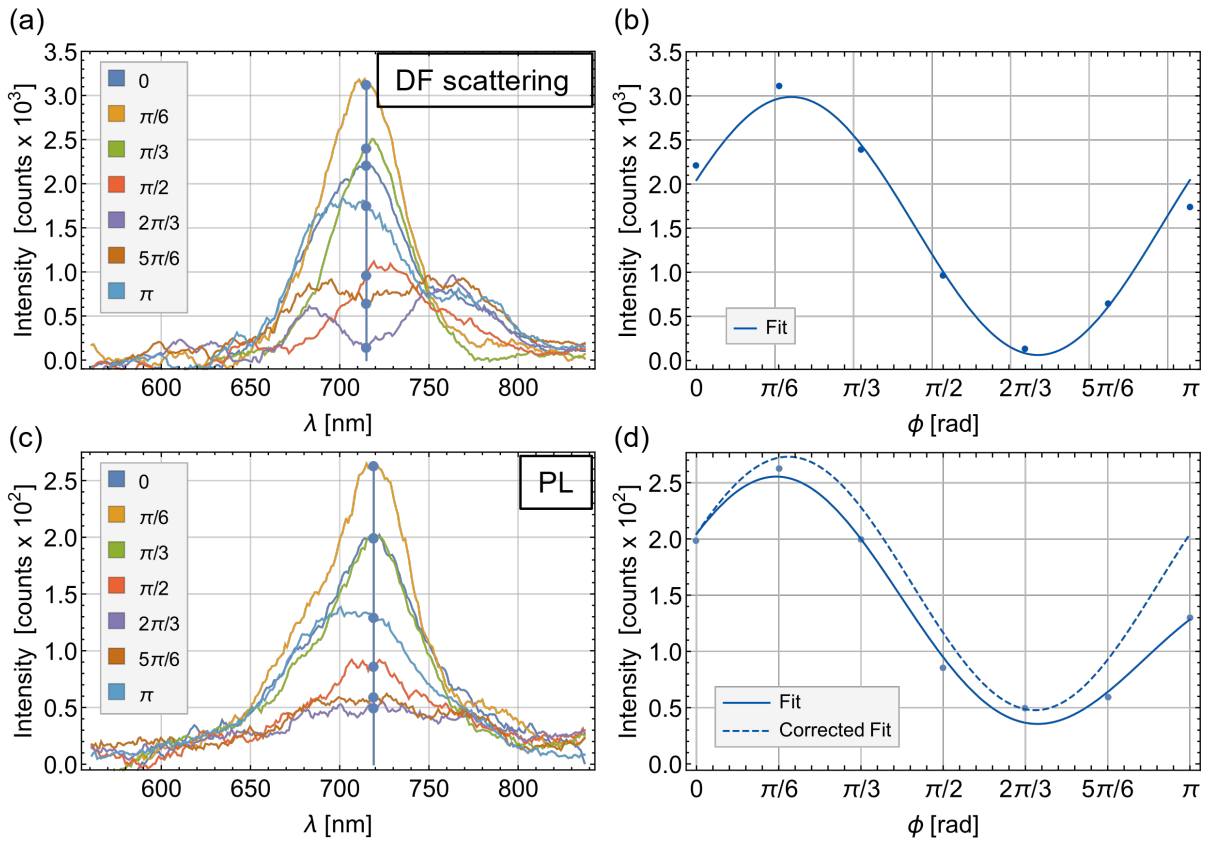


Figure S4: Single particle measurement of (a), (b) DF scattering and (c), (d) PL spectra from AuNRs@AuNCs for different polarizations. AuNRs 1 with 12.5 nm silica shells were used. Peak values from (a) and (c) are plotted as a function of polarization in (b) and (d) respectively to visualize the same polarization dependency of PL and DF scattering for the observed peak at 718 nm. Due to the relatively weak signal collected from the isolated particles, long exposure times had to be used in PL measurements which caused gradual attenuation of the PL intensity. The fitting function ( $\sim \cos^2(\phi)$ ) has been extended with a linear decay term to account for this effect (solid line in d). Removing the linear decay from the fit (dashed line in d) enables better comparison with the DF scattering fit (in b).

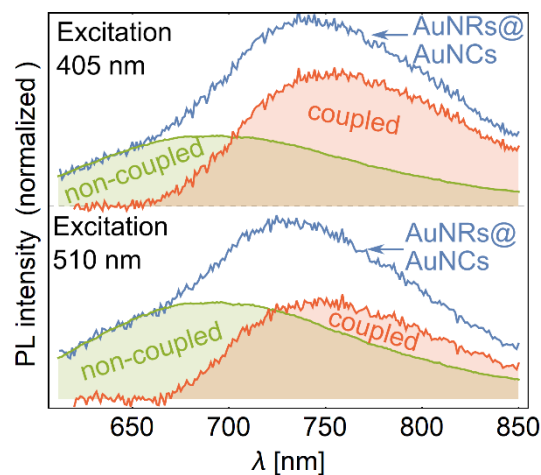


Figure S5: Comparison of PL spectra shapes of AuNRs@AuNCs (5 nm shell) measured at excitation wavelengths 405 nm and 510 nm. An increased contribution from the non-coupled AuNCs is observed for 510 nm excitation compared to 405 nm excitation.

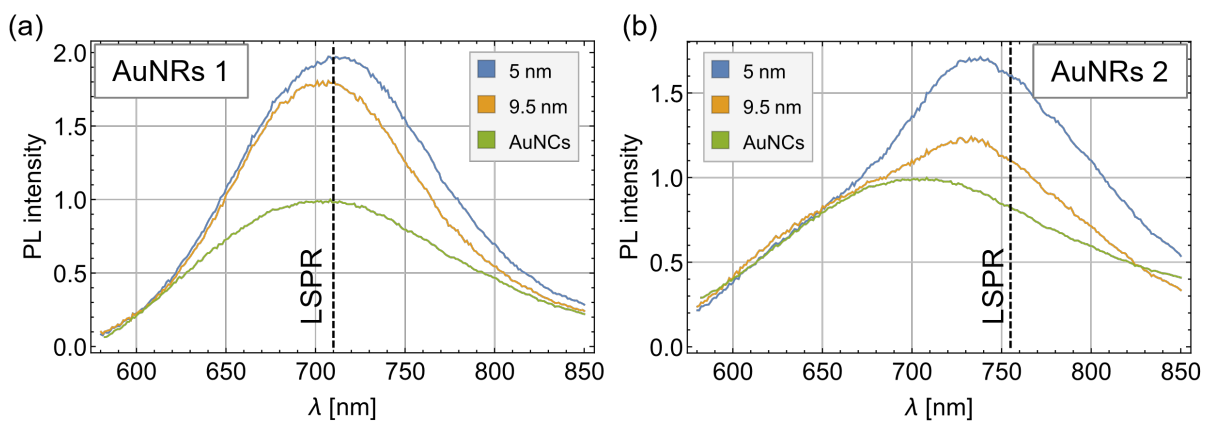


Figure S6: Comparison of the ensemble PL spectra of AuNRs@AuNCs prepared from (a) AuNRs 1 and (b) AuNRs 2. PL spectra of samples with 5 and 9.5 nm shell thickness are compared with the PL spectra of pure AuNCs in both plots. As shown in the experimental part of the manuscript, thinner shells favor stronger contribution from the coupled AuNCs. However, this can be only recognized in (b) where AuNRs with non-perfect PL-LSPR overlap were used.

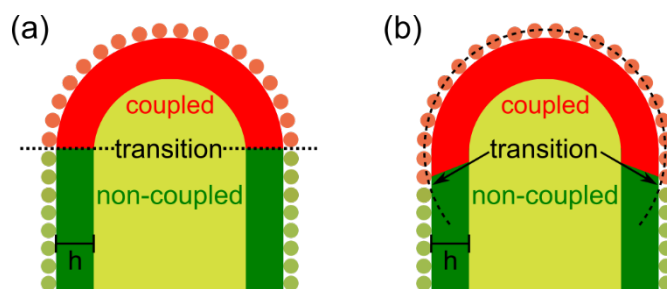


Figure S7: Graphical representation of the model for estimation of the number ratio between coupled and non-coupled AuNCs attached to AuNRs. (a) A simple model used for calculation of the enhancement presented in Figure 6a (in the main text) assumes the transition at the borderline between AuNR tip and body. (b) Alternatively, a model which respects the spherical symmetry of the high Purcell factor area around AuNR tip could be used for example.

### 3. Numerical simulations

#### 3.1. Simulation parameters

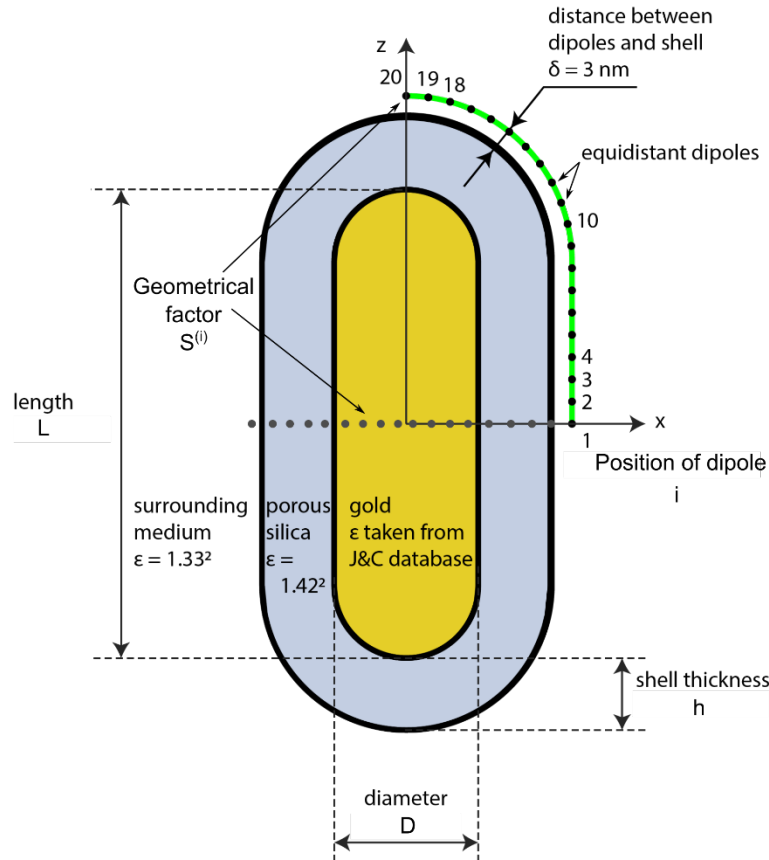


Figure S8: Model of AuNRs@AuNCs used for BEM simulations and notation of input parameters.

The model of AuNRs@AuNCs used for BEM simulations is shown in Figure S8. AuNR is approximated by a cylinder with two hemispherical caps, whose aspect ratio and volume are fully determined by its length ( $L$ ) and diameter ( $D$ ). The silica shell with variable thickness  $h$  is assumed to copy the shape of AuNR. AuNCs are approximated by point dipoles distributed equidistantly on the surface of Au@SiO<sub>2</sub> NR. Due to the symmetry of Au@SiO<sub>2</sub> NRs, the considered positions (denoted by index  $i$ ) are limited to  $\frac{1}{4}$  of the nanorod's perimeter. However, for a correct interpretation of the results of the simulations it is important to realize that the relative contribution of the dipoles with different  $i$  is not the same. On the full surface of Au@SiO<sub>2</sub> NR, there will be considerably more dipoles on the position  $i = 1$  than  $i = 20$  which is reflected by the geometrical factor  $S^{(i)}$ . A constant offset distance between the dipoles and the silica surface is introduced to account for the nonzero physical dimensions of AuNCs and to reduce the computational time. The dielectric function of gold was used from the database of Johnson and Christy<sup>[1]</sup>, the refractive index of porous silica and the surrounding environment was set as 1.42 and 1.33, respectively.

The excitation was simulated as a circularly polarized plane wave travelling perpendicularly to the  $z$ -axis (using the notation from Figure S8). The angle of incidence was varied from along the  $x$ -axis to along the  $y$ -axis from which an average excitation profile was calculated. Such setting best approximates the experimental situation with isolated randomly oriented AuNRs@AuNCs lying on a substrate. Radiative ( $\Gamma_{\text{rad},0}$ ) and nonradiative ( $\Gamma_{\text{nr}}$ ) rates of the dipoles were estimated based on the measured QY (7.8%) and PL lifetime (1.73  $\mu\text{s}$ ) of AuNCs yielding  $\Gamma_{\text{rad},0} = 4.5 * 10^4$  Hz and  $\Gamma_{\text{nr}} = 5.3 * 10^5$  Hz.

Apart from the excitation profile, the core outputs of the simulations are the total and external

Purcell factors ( $f_{\text{tot}}$  and  $f_{\text{ext}}$ ). As shown in the next section, these quantities are sufficient to calculate all the other derived results such as PL lifetime, PL intensity, and PL intensity enhancement. In all cases, these outputs were obtained by averaging the partial results for different dipole positions and orientations ( $x$ -,  $y$ -,  $z$ -), while respecting the geometrical factors  $S^{(i)}$ .

### 3.2. Model

In this study we use the same theoretical model for plasmonic enhancement of PL as we did in one of our previous works<sup>[2]</sup>. To allow for an easier orientation, the derivation of the model's main equations is shown below.

#### Two-level system of nanoparticles

In a two-level system of nanoparticles, the time evolution of concentration (number density) of excited nanoparticles is described by the following differential equation:

$$\frac{dn_2}{dt} = \sigma I_{\text{exc}} n_1 - \Gamma n_2 \quad (3)$$

where  $n_1$  and  $n_2$  are the concentrations of non-excited and excited nanoparticles, respectively,  $I_{\text{exc}}$  is an excitation intensity,  $\sigma$  is an absorption proportionality factor, and the total recombination (decay) rate  $\Gamma$  is a sum of radiative ( $\Gamma_{\text{rad}}$ ) and non-radiative ( $\Gamma_{\text{nr}}$ ) recombination rates. The radiative decay rate depends on particle's dielectric environment and is expressed in terms of a Purcell factor  $f_{\text{tot}}$ :

$$\Gamma = \Gamma_{\text{rad}} + \Gamma_{\text{nr}} = f_{\text{tot}} \Gamma_{\text{rad},0} + \Gamma_{\text{nr}} \quad (4)$$

where  $\Gamma_{\text{rad},0}$  is the radiative decay rate of a nanoparticle in a homogeneous dielectric environment. The Purcell factor has its external and absorbing parts:

$$f_{\text{tot}} = f_{\text{ext}} + f_{\text{abs}} \quad (5)$$

The external part ( $f_{\text{ext}}$ ) is responsible for far-field emission. The absorbing part ( $f_{\text{abs}}$ ) describes electromagnetic losses in a dielectric environment of a nanoparticle such as quenching and absorption. The photoluminescence intensity  $I_{\text{PL}}$  is given by:

$$I_{\text{PL}} = \alpha n_2 f_{\text{ext}} \Gamma_{\text{rad},0} \quad (6)$$

where  $\alpha$  is a proportionality factor.

#### PL intensity enhancement under constant excitation

In a steady state,  $dn_2/dt = 0$  and

$$n_2 = \frac{\sigma I_{\text{exc}} n}{\sigma I_{\text{exc}} + \Gamma_{\text{rad}} + \Gamma_{\text{nr}}} \quad (7)$$

where  $n = n_1 + n_2 = \text{const.}$  is the total concentration of nanoparticles. Using (4) and (6) we get for the PL intensity:

$$I_{\text{PL}} = \frac{\alpha \sigma n I_{\text{exc}} f_{\text{ext}} \Gamma_{\text{rad},0}}{\sigma I_{\text{exc}} + \Gamma_{\text{nr}} + f_{\text{tot}} \Gamma_{\text{rad},0}} \quad (8)$$

In case of a weak excitation ( $\sigma I_{\text{exc}} \ll \Gamma$ ) we can write:

$$I_{PL} = \alpha \sigma n I_{exc} \frac{f_{ext} \Gamma_{rad,0}}{\Gamma_{nr} + f_{tot} \Gamma_{rad,0}} \quad (9)$$

Using (9) and by setting  $f_{ext} = f_{tot} = 1$ , we get the expression for PL intensity of pure nanoparticles (AuNCs):

$$I_{PL,0} = \alpha \sigma n I_{exc,0} \frac{\Gamma_{rad,0}}{\Gamma_{nr} + \Gamma_{rad,0}} = \alpha \sigma n I_{exc,0} \eta_0 \quad (10)$$

Where  $I_{exc,0}$  is the excitation intensity acting on the nanoparticles without plasmonic enhancement and  $\eta_0$  is the original quantum yield of the nanoparticles. Substituting for  $n$  from (10) to (9) we get:

$$I_{PL} = \frac{1}{\eta_0} \frac{I_{exc}}{I_{exc,0}} I_{PL,0} \frac{f_{ext} \Gamma_{rad,0}}{\Gamma_{nr} + f_{tot} \Gamma_{rad,0}} \quad (11)$$

Note that this expression is only valid for a single dipole with fixed position, orientation and incidence of the excitation light. To get the correct result,  $I_{exc}$ ,  $f_{ext}$ , and  $f_{tot}$  must be averaged. Moreover, to get the actual spectrum,  $I_{PL,0}$  and the Purcell factors are considered as a function of wavelength ( $I_{PL,0}(\lambda)$ ,  $f_{ext}(\lambda)$ ,  $f_{tot}(\lambda)$ ). The lineshape of pure AuNCs was assumed to be gaussian:

$$I_{PL,0}(\lambda) = I_0 e^{-\frac{(\frac{hc}{\lambda} - E_0)^2}{2\omega^2}} \quad (12)$$

where  $E_0 = 1.771$  eV and  $\omega = 0.18$  eV determine the central wavelength and width of the peak, respectively. This choice is justified by a good agreement between the theoretical and experimental emission peak shown in Figure S9.

Finally, the PL enhancement factor can be found straightforwardly from (11) as:

$$\xi = \frac{I_{PL}}{I_{PL,0}} = \frac{1}{\eta_0} \frac{I_{exc}}{I_{exc,0}} \frac{f_{ext} \Gamma_{rad,0}}{\Gamma_{nr} + f_{tot} \Gamma_{rad,0}} \quad (13)$$

The last part of this expression is actually the modified quantum yield of the nanoparticles:

$$\eta = \frac{f_{ext} \Gamma_{rad,0}}{\Gamma_{nr} + f_{tot} \Gamma_{rad,0}} \quad (14)$$

and (13) can be thus further rewritten as:

$$\xi = \frac{I_{exc}}{I_{exc,0}} * \frac{\eta}{\eta_0} = \xi_{exc} * \xi_{QY} \quad (15)$$

where  $\xi_{exc}$  is the excitation enhancement and  $\xi_{QY}$  is the quantum yield enhancement. Note that the overall PL intensity from all dipoles is obtained by averaging their partial contributions weighed by the corresponding geometrical factors  $S^{(i)}$  as discussed in the section 3.1.

### PL decay rate enhancement under pulsed excitation

Under pulsed excitation, the time evolution of PL from NCs located at the  $i$ -th position is set by equation (6) and has the form:

$$I_{PL}^{(i)}(t) = \alpha f_{ext}^{(i)} \Gamma_{rad,0} * n_{2,0}^{(i)} e^{-\Gamma^{(i)} t} \quad (16)$$

The initial concentration of excited NCs at the  $i$ -th position ( $n_{2,0}^{(i)}$ ) is proportional to the excitation intensity at this position and thus:

$$I_{PL}^{(i)}(t) = \alpha \beta I_{exc}^{(i)} f_{ext}^{(i)} \Gamma_{rad,0} e^{-\Gamma^{(i)} t} \quad (17)$$

where  $\beta$  is the proportionality factor. The average decay rate is found as a weighted arithmetic mean, where the weight of the corresponding geometric factors  $S^{(i)}$  has to be again considered:

$$\Gamma^{ave} = \frac{\sum_i I_{exc}^{(i)} f_{ext}^{(i)} S^{(i)} \Gamma^{(i)}}{\sum_i I_{exc}^{(i)} f_{ext}^{(i)} S^{(i)}} = \Gamma_{nr} + \Gamma_{rad,0} f_{tot}^{ave} \quad (18)$$

where  $f_{tot}^{ave}$  is the average Purcell factor:

$$f_{tot}^{ave} = \frac{\sum_i I_{exc}^{(i)} f_{ext}^{(i)} S^{(i)} f_{tot}^{(i)}}{\sum_i I_{exc}^{(i)} f_{ext}^{(i)} S^{(i)}} \quad (19)$$

and  $f_{tot}^{(i)}$  is the total Purcell factor of a dipole located at the  $i$ -th position.

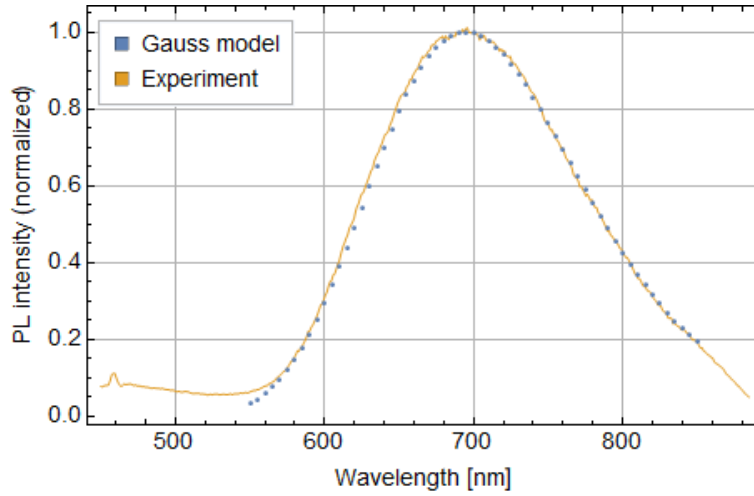


Figure S9: A comparison of the normalized PL intensity of AuNCs as measured experimentally and as approximated for calculation of the simulated spectra.

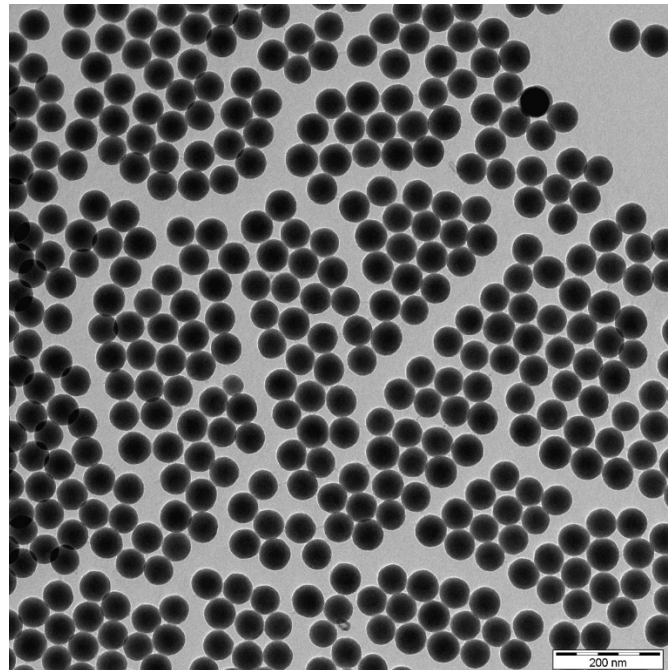


Figure S10: TEM micrograph of the monodisperse spherical  $\text{SiO}_2$  nanoparticles used for preparation of  $\text{SiO}_2\text{NPs@AuNCs}$ .